



Predictive GT-Power Simulation for VNT Matching on a 1.6 L Turbocharged GDI Engine

Dennis Robertson, Graham Conway, and Chris Chadwell Southwest Research Institute

Joseph McDonald, Daniel Barba, and Mark Stuhldreher US Environmental Protection Agency

Aaron Birckett Honeywell Transportation Systems

Citation: Robertson, D., Conway, G., Chadwell, C., McDonald, J. et al., "Predictive GT-Power Simulation for VNT Matching on a 1.6 L Turbocharged GDI Engine," SAE Technical Paper 2018-01-0161, 2018, doi:10.4271/2018-01-0161.

Abstract

The thermal efficiency benefits of low-pressure (LP) exhaust gas recirculation (EGR) in spark-ignition engine combustion are well known. One of the greatest barriers facing adoption of LP-EGR for high power-density applications is the challenge of boosting. Variable nozzle turbines (VNTs) have recently been developed for gasoline applications operating at high exhaust gas temperatures (EGTs). The use of a single VNT as a boost device may provide a lower-cost option compared to two-stage boosting systems or 48 V electronic boost devices for some LP-EGR applications. A predictive model was created based on engine testing results from a 1.6 L turbocharged gasoline direct injection

(GDI) engine [1]. The model was tuned so that it predicted burn-rates and end-gas knock over an engine operating map with varying speeds, loads, EGR rates and fuel types. Using the model, an assessment of VNT performance was performed using compressor and turbine maps made available from Honeywell Transportation Systems. Results show that the single VNT device supports LP-EGR across the operating map while maintaining realistic full-load performance and maintaining or improving upon thermal efficiency compared to a twin-scroll turbocharger. This work was done as part of the Environmental Protection Agency's continuing assessment of advanced light-duty automotive technologies to support setting appropriate national greenhouse gas standards.

Introduction

By 2025, the automotive industry must reduce CO₂ emissions by at least 30% and criteria pollutant emissions for vehicles sold in the U.S. by a factor of three [2]. To achieve these emissions standards, advanced engine combustion strategies are being pursued. One promising strategy is the use of cooled exhaust gas recirculation (EGR) [3, 4, 5, 6].

Cooled EGR leads to higher thermal efficiencies through a reduction in heat transfer losses. Cooled EGR is also well known to improve knock resistance, enabling either higher compression ratios or increased specific torque with optimal combustion phasing. Additionally, cooled EGR offers benefits relative to specific heat by displacing the diatomic air molecules with triatomic molecules recirculated from the exhaust. The increase in heat capacity reduces combustion temperatures, leading to lower NO_x and CO emissions [7]. Finally, pumping losses decrease with the use of cooled EGR by reducing the volumetric efficiency of the engine and requiring higher manifold pressure for a given load.

However, greater use of cooled EGR introduces a challenge in the sizing of traditional turbochargers. The turbine in a traditional single-stage turbocharger is size-compromised to achieve the low-speed, high-load target as well as a high enough flow capacity for minimized turbine inlet pressure at

the rated power condition. The two performance targets require a design trade-off between low- and high-speed torque performance, resulting in a less than optimum turbine size for either condition.

Variable nozzle turbines (VNTs) have the benefit of being able to adjust their turbine geometry to allow an effectively smaller turbine diameter at low speed (to achieve low-end torque) and an effectively larger turbine diameter at high speed (to achieve lower back pressure and high-power performance) [8, 9]. An added benefit of reduced exhaust back pressure at high engine loads is that it avoids the need for a wastegate. This reduction in exhaust backpressure is beneficial as it lowers the scavenging pressure ratio, which reduces the residual content in-cylinder and allows earlier combustion phasing and improved engine efficiency [10]. Previous studies have shown the success of VNT with Miller operation. This paper identifies the potential of VNT to operate under dilute conditions, specifically EGR dilution.

The purpose of this work was to develop an engine model using Gamma Technologies' GT-Power software (Gamma Technologies, LLC., Westmont, IL) with a predictive combustion mechanism. This model assessed the performance of a VNT's ability to support low pressure LP-EGR across the engine operating map and its impact on thermal efficiency with varying EGR rates and fuel types. To accurately model

FIGURE 1 EP6CDTx engine.

US Government / US Environmental Protection Agency

TABLE 1 PSA EP6CDTx Specifications.

Displacement	1.6 L
Bore	77 mm
Stroke	85.8 mm
CR	10.5:1
Turbocharger	Original equipment twin-scroll or VNT
E-Boost	Boost cart with supercharger
Valve train	Intake and Exhaust Cam Phaser Intake Valvetronic (Continuous VVL)
Injection system	Side-mounted GDI
Rated Power	120 kW @ 5000 rpm
Rated Torque	240 Nm @ 1600–4000 rpm

US Government / US Environmental Protection Agency

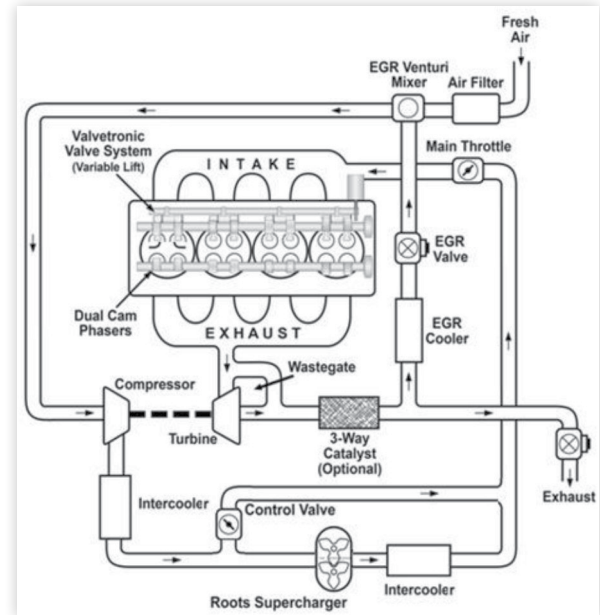
the effects of varying exhaust residuals, boost pressure and spark timing, a predictive, quasi-dimensional combustion model was constructed within GT-Power using data from an experimental version of a production PSA (Peugeot Société Anonyme) 1.6 L turbocharged engine shown in [Figure 1](#) and [Table 1](#).

The output from the quasi-dimensional combustion model was used to investigate the effect of cooled EGR on inhibiting autoignition in a downsized turbocharged engine. In addition, further model data are presented demonstrating the capability of the model to predict boosting requirements correctly for a VNT or twin-scroll turbocharger at rated power.

Simulation Model

The engine selected for this study was a PSA EP6CDTx configured with LP-EGR [1]. [Table 1](#) lists the engine geometry and test configuration, and [Figure 1](#) depicts the engine.

Supplemental boost was required when the twin-scroll turbocharger was unable to meet the target load at the desired EGR rate. To supply the supplemental boost, a mechanical supercharger coupled to an electric motor was

FIGURE 2 Engine configuration as found in test-cell and as modelled within GT-Power. Boost is provided via stock, twin-scroll turbocharger and added positive displacement supercharger. The EGR valve is placed post-EGR cooler downstream of the turbine.

US Government / US Environmental Protection Agency

used. A schematic of the test cell setup can be found in [Figure 2](#). While electrical power consumed by the supercharger electric motor was not included in the analysis, its operation and expected backpressure were included. The exhaust manifold pressure was increased to match the intake manifold pressure to simulate a turbocharger capable of meeting the boost pressure requirement. For all simulated conditions, the manifold air temperature was set to 40 °C to align with the engine testing. The post-turbine EGR was routed to the intake without passing through a three-way-catalyst (TWC). The EGR therefore has uncatalyzed HC, CO and lesser amounts of H₂ and these can all help the dilute combustion process by increasing the flame speed [11]. Further details of the test setup can be found in the companion paper [1].

Model Geometry

The test engine was modeled in GT-Power (Gamma Technologies, Ltd., Morrisville, NC, USA). Component geometry was determined with a combination of direct measurement, engineering judgment, or was provided by the component manufacturer (see [Table 2](#)).

To achieve the objectives of this study, the GT-Power model required the following features:

- Predictive combustion
- Predictive knock
- Cycle-by-cycle adjustment of combustion phasing to mitigate knock per the knock model prediction
- Flexible load control algorithm

TABLE 2 Sources of geometry data.

Model Component	Method
Intake, Exhaust, and EGR Systems	Direct measurement
Valve Flow Coefficients	Flow Bench Testing
Cylinder	Engineering Estimate Provided by Manufacturer
Turbocharger and External Boost Device	Provided by Supplier

FIGURE 3 10:5:1 combustion chamber surface geometry.



Predictive combustion models require detailed topography of the in-cylinder geometry to predict wetted flame area and turbulence. Non-predictive models such as the Wiebe function [12, 13, 14] rely primarily on test data. Head and piston surface models were added to the engine model by importing stereolithography (STL) files of the piston and cylinder head surfaces that represent the combustion chamber. (Figure 3) illustrates the piston and cylinder head surface geometries used as input to the model. The surface detail was coarsened to speed computation times by setting the *Surface Discretization Resolution* parameter to 1.0. The network of pipes that make up the engine breathing system were imported from CAD models by converting STL files into GT-Power map parts using GT-Power’s GEM3D software.

Load Control

The model was designed to operate across the baseline speed and load map of the engine with varying EGR rates, different fuels, and moderate hardware changes. The load control algorithm must both be flexible and mimic the baseline calibration of the engine. The selected load control algorithm was a state machine and can be seen in Table 3.

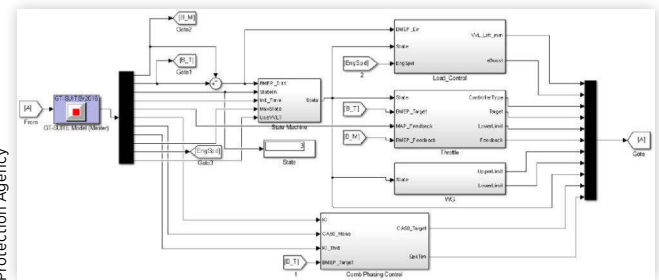
This control algorithm was implemented in the GT-Power model via Mathworks (Natick, MA) MATLAB Simulink co-simulation. Co-simulation enabled the combined advantages of GT-Power controllers and Simulink capability to offer a flexible and robust control architecture. The state machine and combustion phasing logic was entirely coded in Simulink. The throttle and turbocharger controllers in GT-Power are robust, as they are model-based. The Simulink code, therefore, only configured these controllers to operate in the desired state. This configuration was achieved by setting targets and limits for the GT-Power controllers from the Simulink code.

The complete Simulink code is illustrated in Figure 4. The code was compiled as a dynamic link library file (.dll extension) and input in the GT-Power model via the *SimulinkHarness*

TABLE 3 Load control algorithm.

State	Load Control Device	Remaining Load Control Actuator Positions
0	Variable valve lift (VVL), throttle targeted 92 kPa intake manifold pressure	Wastegate wide open External boost device fixed at 0 RPM
1	Throttle	VVL set to maximum lift Wastegate wide open External boost device fixed at 0 RPM
2	Wastegate	VVL set to maximum lift Throttle wide-open External boost device fixed at 0 RPM
3	External Boost Device	VVL set to maximum lift Throttle wide-open Wastegate closed

FIGURE 4 Simulink control code. A larger-scale version of this schematic is reproduced within Appendix Figure 1 for improved legibility.



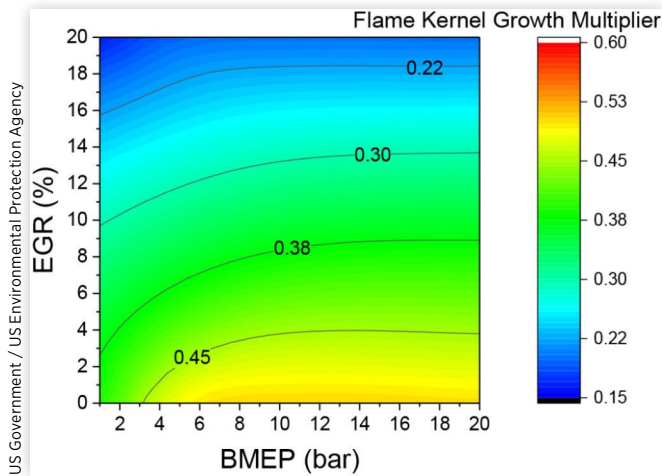
object (Figure 5). Engine measurements, controls, and monitors interfaced with this object in the GT map.

Predictive Combustion (SITurb)

Predictive combustion modeling was included to predict combustion performance across the wide range of operating conditions, an important consideration when adjusting engine back pressure, as experienced by a boosting device study. When changing back pressure, total trapped residual content changes. The presence of residual content will affect burn rates, autoignition, heat transfer and effective volumetric efficiency. The *SITurb* model within GT-Power has the capability to account for the above processes and was selected for this boosting device study.

Combustion in spark-ignition gasoline engines is premixed turbulent combustion. The flame begins from exothermic reactions ignited by the high temperature ignition kernel. The reactions form a laminar-like flame which is then wrinkled and perturbed by varying scales of turbulence, primarily the Taylor microscale [15]. During this phase, the flame is defined as a *developing flame*. Once the flame has grown to a size larger than the integral scale of turbulence,

FIGURE 9 Tuning map for Flame Kernel Growth Multiplier.



start of combustion between the predictive model and the test data. The primary tuning parameter was FKGM. Start of combustion has a minimal impact on performance or combustion, but it does provide an indication of the required spark advance.

Knock Model

A knock model was developed to identify a reasonable combustion phasing for the controller to target. The knock model must predict knock over the full range of speeds and loads with varying EGR rates.

The knock model used is based on the Livengood and Wu induction time integral (Eq. 1) [16] and uses the Douaud and Eyzat (D&E) empirical model (Eq. 2) [17] to calculate autoignition delay times. Once the integral reaches unity, autoignition is deemed to occur. The D&E model considers only pressure and temperature of the end-gas. The role of dilution in chemical kinetics must be accounted for by adjustment of the *Activation Energy Multiplier*. The nature of this model requires an ad hoc approach to EGR knock modeling—a significant limitation to the broad application of the model. At the time of the analysis, Gamma Technologies had developed a chemical kinetics-based knock model called *kinetics-fit-gasoline* knock model; however, it was still considered experimental in GT-Power v2016, and thus was not used.

$$\int_{t=0}^{t_a} \frac{dt}{\tau} = 1 \tag{1}$$

$$\tau = 17.68 \left(\frac{ON}{100} \right)^2 P^{-1.7} e^{\left(\frac{3800}{M \cdot T} \right)} \tag{2}$$

Where:

- ON = Research Octane Number
- P = Pressure
- T = Temperature
- M = Activation Energy Multiplier
- τ = Autoignition Delay Time

The octane number was matched to the anti-knock index (AKI) of the test fuel, and the activation energy was tuned to

the test data. The knock model was calibrated to test data by tuning the Activation Energy Multiplier as a function of speed and EGR rate, (Figure 10). Without a chemical kinetics component, the knock tolerance benefit of EGR must be affected by a lower *Activation Energy Multiplier*.

The knock model was exercised at 2000 RPM and 10 bar BMEP. With the baseline compression ratio (CR), this point was the maximum load at minimum spark advance for best torque (MBT) timing. Knock onset was considered at a knock index of 5. Knock index is sensitive, thus any value from 5–10 was considered knock onset. The difference in the knock-limited CA50 (the point at which 50% of the fuel is burned) from a knock index of 5 to 10 was ~0.5°.

A compression ratio increase of 1.3 points was investigated. The knock model predicted an increase in knock. Various knock mitigation techniques were applied: later combustion phasing, EGR dilution, and higher AKI fuel. Each knock mitigation technique sufficiently eliminated knock. (Figure 11) provides a visual for the cylinder pressure with the increased compression ratio and the knock mitigation techniques. Table 4 gives numerical values for the critical parameter changes.

FIGURE 10 Map of Activation Energy Multiplier.

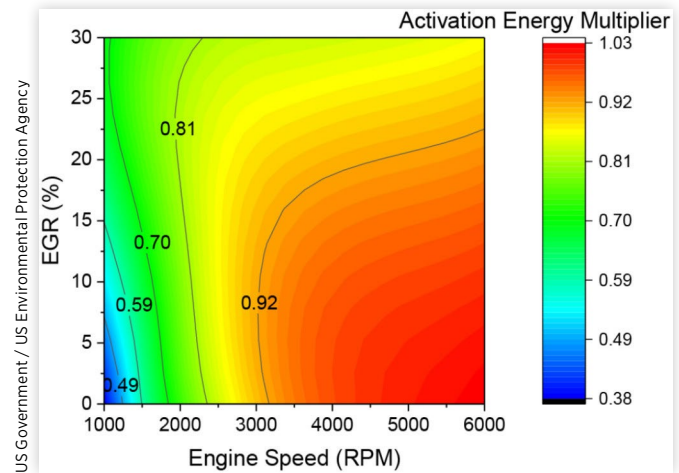


FIGURE 11 Cylinder pressure progression through knock mitigation strategies.

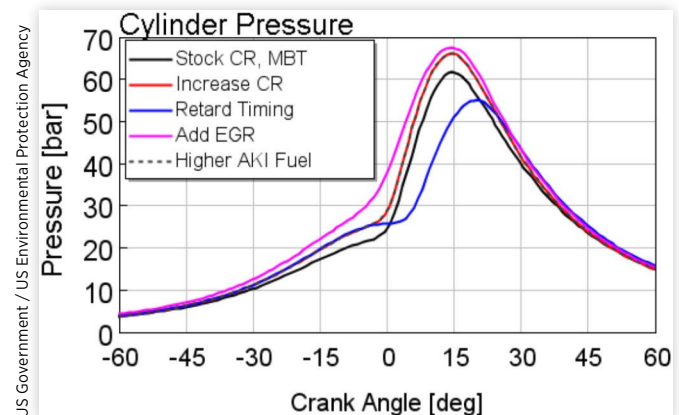


TABLE 4 Configuration and knock performance of the knock mitigation strategies.

	CR	CA50 [°aTDC]	EGR [%]	Fuel AKI	Knock Index
Base CR, MBT	10.5	8	0	93	9.4
Increase CR	11.8	8	0	93	95.0
Retard Timing	11.8	13	0	93	7.7
Add EGR	11.8	8	18	93	6.7
High AKI Fuel	11.8	8	0	100	13.2

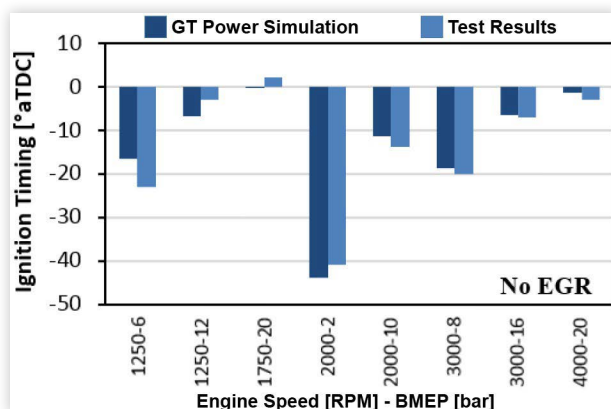
US Government / US Environmental Protection Agency

Validation to Test Data

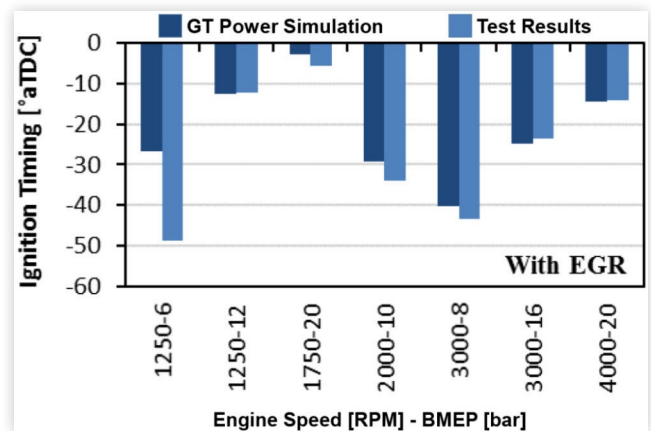
As outlined in Conway et al. [1], the engine generated data for over 200 test conditions with and without LP-EGR. Data generated at these points was used to validate the GT-Power model created for this study. Eight points were selected for an initial validation. These points cover a wide operating portion of the engine map and give an indication of the performance of the GT-Power model under all conditions. A comparison of the ignition timing for conditions with and without LP-EGR can be seen in Figure 12 and Figure 13. Ignition timing was adjusted to target comparable CA50. Except for 1250 RPM and 6 bar BMEP, all conditions match well both with and without LP-EGR.

MFB 10–90 is the other tuned parameter, and a comparison between test data and simulation results is presented in Figure 14 and Figure 15. The primary tuning parameter for MFB 10–90 was the TFSM. Comparing all cases identifies that the model under-predicts the burn rates, that is, the predicted MFB 10–90 are longer than the test data, although there are cases where the trend is reversed. It would be possible to individually tune the TFSM for each individual case, however this would remove any predictive capability from the model.

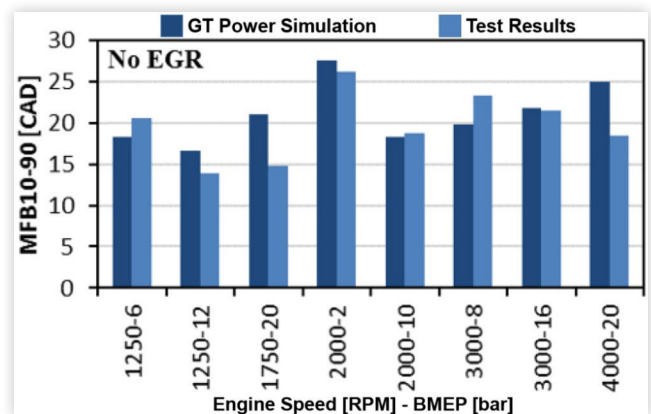
As well as the MFB 10–90 duration being matched, it is necessary to match the combustion process from spark to termination. A comparison between simulated and experimental shape of the MFB curve under two different sets of conditions can be seen in Figure 16 where there is good agreement between prediction and test data.

FIGURE 12 Start of combustion validation without EGR.

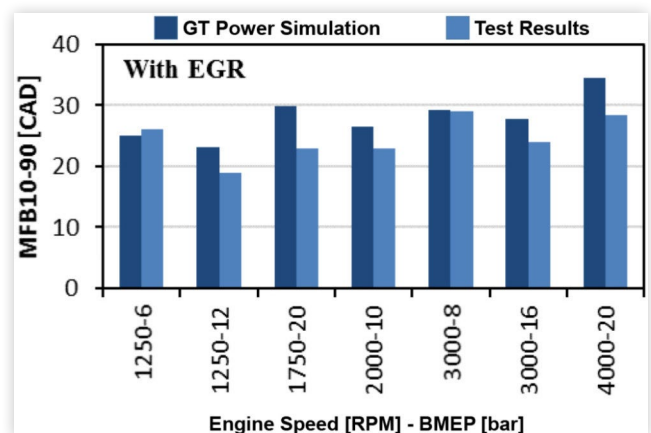
US Government / US Environmental Protection Agency

FIGURE 13 Start of combustion validation with EGR.

US Government / US Environmental Protection Agency

FIGURE 14 Burn duration validation without EGR.

US Government / US Environmental Protection Agency

FIGURE 15 Burn duration validation with EGR.

US Government / US Environmental Protection Agency

The knock model matched test data within -3° to $+3^\circ$ CA50 along the lug curve (Figure 17). Improving the accuracy of the model would require a point-by-point adjustment of the Activation Energy Multiplier. This approach was not desirable as it would hinder the predictive capability of the model.

Predictive simulations were performed across the operating map under more than 70 speeds–load conditions; the

FIGURE 16 MFB curve at 2000-2 and 3000-20 without EGR.

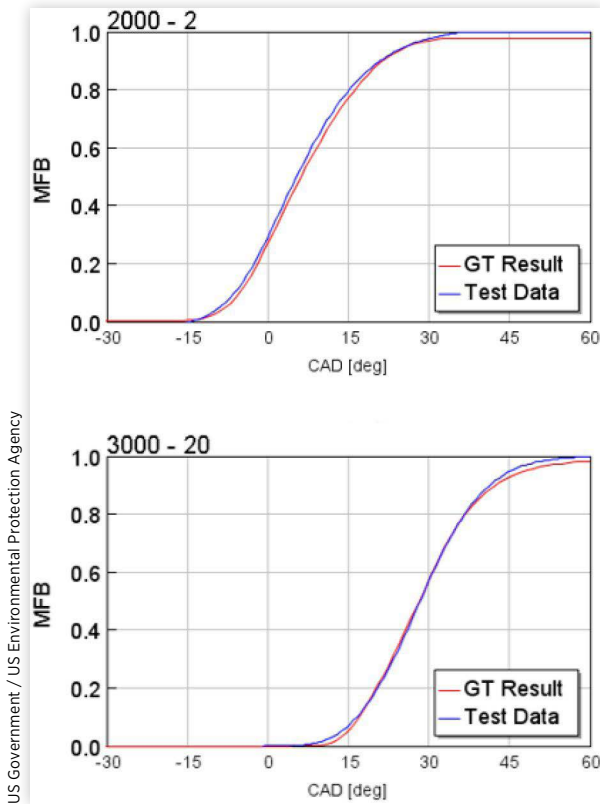
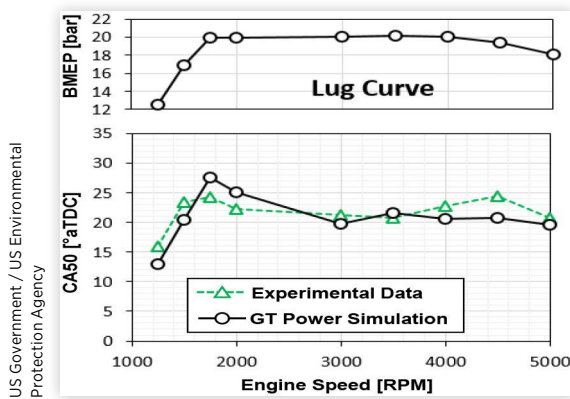


FIGURE 17 Knock model performance compared to test data across the lug curve.



predicted brake specific fuel consumption (BSFC) results can be seen in [Figure 18](#).

The predicted BSFC values were compared to test data run using an external boost device and twin-scroll turbocharger. The average BSFC error compared to test data was below 2% over the operating area of the map as can be seen in [Figure 19](#). At loads below 1 bar BMEP, BSFC is highly sensitive to friction and pumping. The Chen-Flynn friction model [18] used within GT-Power was tuned to motoring data but not to fired data and therefore may not accurately represent the true physics. In knock-limited areas, the model predicts higher BSFC than observed during testing. BSFC prediction

FIGURE 18 BSFC results from GT-Power simulation with EGR.

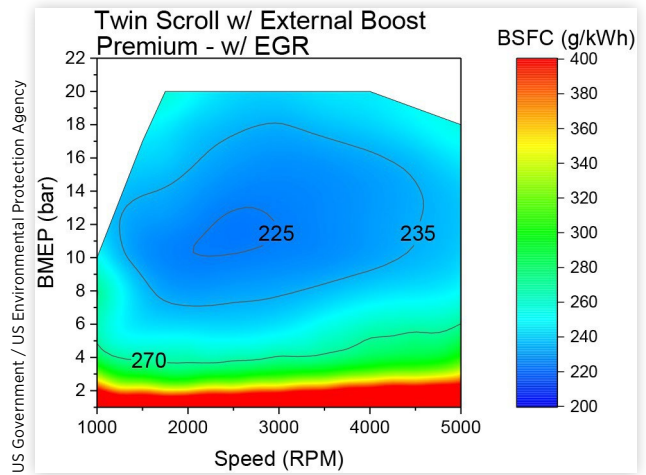
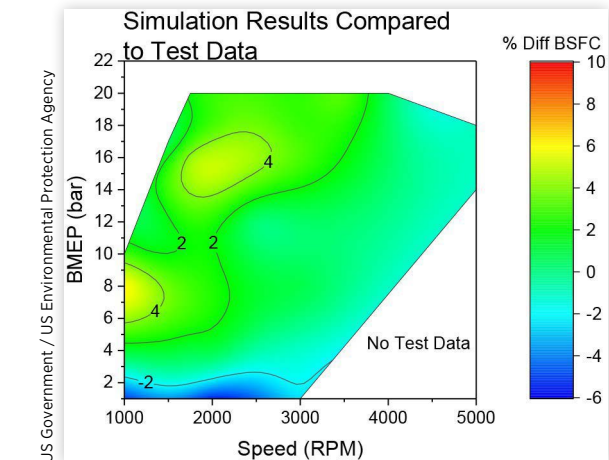


FIGURE 19 BSFC difference between test data and the final GT-Power simulation. Positive values suggest that predicted BSFC values were higher than test data.



here is subject to the predictive capability of the D&E knock model. An overprediction of knock will result in combustion phasing retardation and an increase in BSFC.

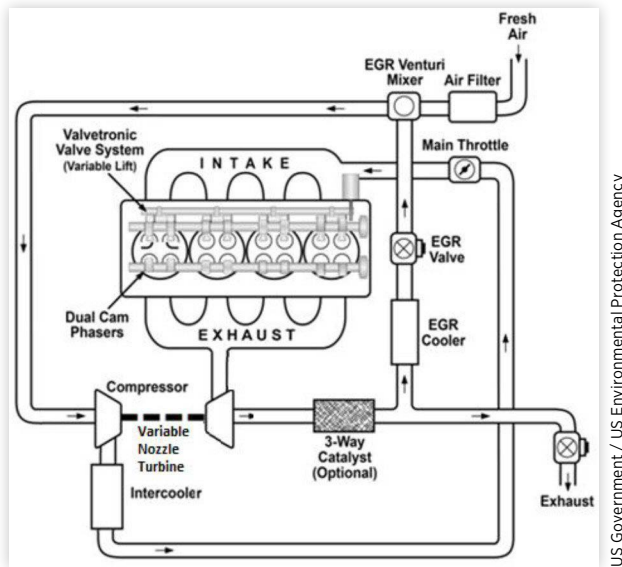
VNT Simulation

After the model was validated against the twin-scroll test data, the VNT turbocharger maps from Honeywell Transportation Systems¹ were included in the model. The new configuration modeled within GT-Power can be seen in [Figure 20](#). Note the removal of the wastegate and supercharger device.

The process to select the gasoline specific VNT map is independent of the compressor map. The first step is assuming that the compressor corrected mass flow and pressure ratio would remain the same and therefore only the turbine map is changed from the twin-scroll to VNT. Further compressor

¹ Honeywell Transportation Systems, Plymouth, MI/Rolle, Switzerland is a major supplier of automotive turbochargers.

FIGURE 20 Engine as configured in GT-Power using a VNT boost device. The supplement boost is removed for this configuration.

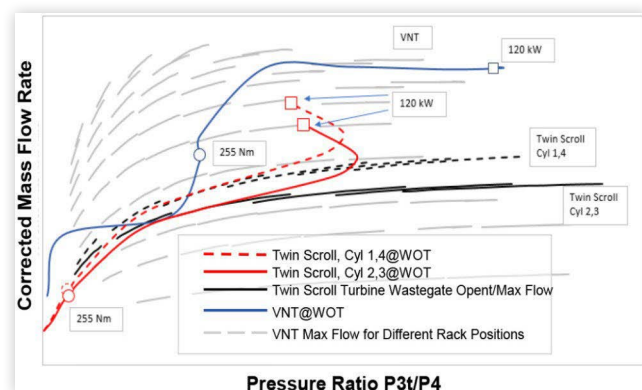


US Government / US Environmental Protection Agency

map iteration can be conducted once the ideal VNT turbine is selected. The VNT is selected such that it has sufficient mass flow capacity to cover the low speed torque region (VNT in more closed position) to the high speed rated power point (VNT more open to reduce turbine inlet pressure and power). The twin-scroll turbine has a wastegate valve used to bypass excess turbine energy to control the compressor to a specific mass flow and pressure ratio. A properly matched VNT should not need the wastegate valve as the map width is tailored to contain all the engine operating points. (Figure 21) shows the full load curve on both the twin-scroll and VNT turbines.

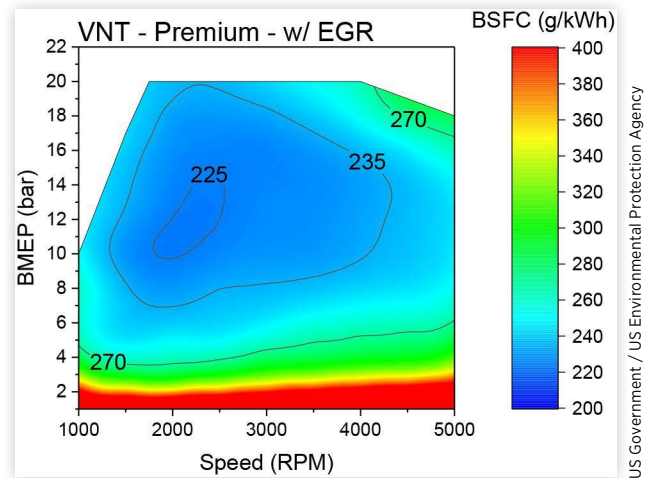
The predictive combustion and knock from the twin-scroll model were maintained with no adjustment. Any change in back pressure would still be accounted for by the predictive models, but no further calibration effort was required. The same engine actuator positions were also maintained, except where noted. The BSFC map for the VNT model is illustrated in Figure 22.

FIGURE 21 Turbine operation along full load curve, twin-scroll and VNT (courtesy of Honeywell Transportation Systems – units removed at the request of the manufacturer).



US Government / US Environmental Protection Agency

FIGURE 22 BSFC map for VNT hardware with EGR.

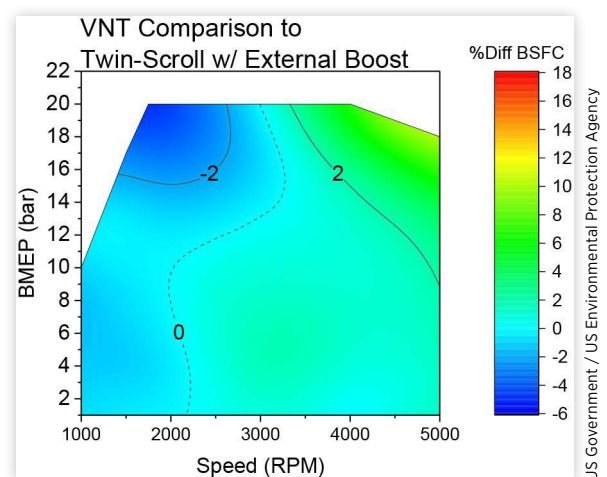


US Government / US Environmental Protection Agency

Below 12 bar BMEP, the VNT BSFC was like the twin-scroll with external boost, where boosting was not significant. For low-speed (e.g., below 2500 RPM) and high-load (e.g., above 15 bar BMEP), improved knock resistance and pumping work from lower backpressure yielded improved fuel efficiency with the VNT. At high power, the VNT results indicated higher BSFC from increased backpressure due to the smaller turbine. The increase in back pressure led to higher trapped residuals and higher knock potential. In reaction to the onset of knock, ignition timing was retarded, thus reducing efficiency. Additionally, at high loads and engine speeds, exhaust gas temperature limits become critical and it was necessary to add additional fuel to cool the exhaust gas, again to the detriment of efficiency. Recall, the twin-scroll turbocharger required supplemental boost at low speeds. A BSFC percentage difference map between the VNT and twin-scroll with external boost is pictured in Figure 23.

The compressor operation over full load is depicted in Figure 24. The margin of compressor surge at the left-hand side of the map and choke margin towards the right-hand side are within the acceptable limits defined by Honeywell (Figure 24). To achieve a targeted load, the EGR rate was reduced (Figure 25) as load was increased. At speeds below 1750 RPM, the required

FIGURE 23 Difference map of BSFC comparing the VNT and twin-scroll (with external boost).



US Government / US Environmental Protection Agency

FIGURE 24 Compressor operation along full load curve. (courtesy of Honeywell Transportation Systems - x-y units removed at the request of the manufacturer).

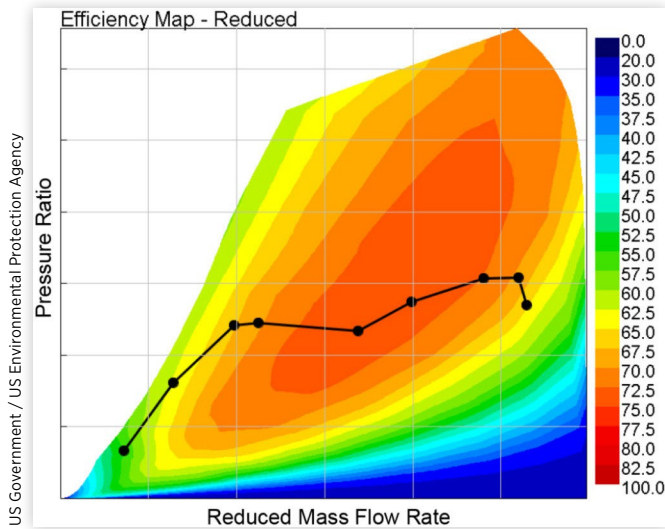
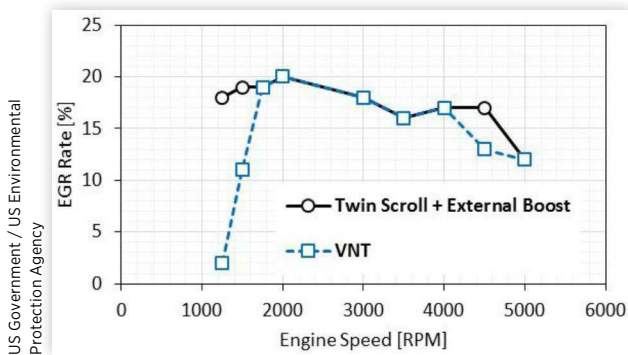


FIGURE 25 EGR rate comparison between VNT and twin-scroll (with external boost).



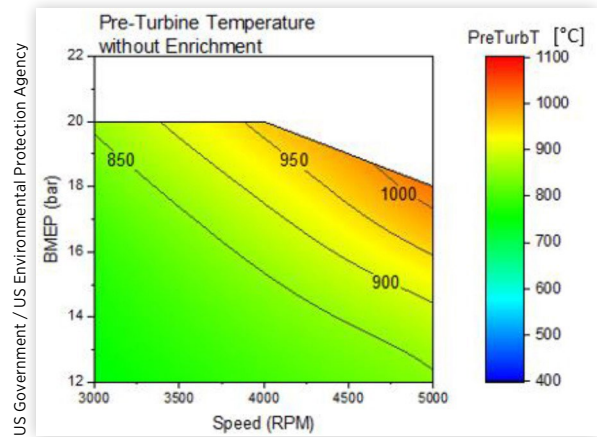
boost pressure to achieve the target load with EGR exceeded the capability of the VNT. The lower dilution at high power raised exhaust temperatures enough to require fuel enrichment to maintain <950 °C pre-turbine temperature.

A pre-turbine temperature map, without enrichment, is illustrated in Figure 26. This map shows pre-turbine temperature if no enrichment were used. The maximum exhaust temperature predicted was 1020 °C.

Overall, the model predicted that VNT would perform as well as a single boost device. The model predicted that reduced EGR rates would be required to achieve targeted loads at low and high speeds. There was minor change in BSFC across much of the map and it was possible to meet the target torque curve, albeit with reduced efficiency, at the high power.

Emissions performance and fuel efficiency suffered at peak power from enrichment for component protection. Pre-turbine temperatures were maintained at <950 °C. EGR rate was reduced at 4500 RPM to meet performance targets. To avoid enrichment at the same power, the turbine must be capable of 1020 °C turbine inlet temperatures or a modified turbine size must be found that reduces back pressure sufficiently at high loads to be able to utilize EGR to reduce exhaust gas temperature.

FIGURE 26 Pre-turbine temperature map near rated power without enrichment.



Regular Grade Fuel Analysis

The initial fuel chosen for the GT-Power simulation was the EPA Tier II ‘Premium’ fuel. For the second phase of testing, the LEV III ‘Regular’ fuel with 10% ethanol, by volume, from the California Low Emissions Vehicle Program (LEV) was used [19]. Specifications for each fuel can be seen in Table 5.

The fuel used for the initial engine simulation runs was the Tier 2 certification fuel, (like a premium grade fuel) to align with the test data. Until recently, vehicle emission certification and compliance testing in the U.S. used a premium quality fuel with approximately 93AKI and no added ethanol (E0). However, the Tier 3 and LEV III fuels now used for criteria pollutant emissions compliance consist of both a low and a high AKI and are formulated to match the average ethanol (E10) and aromatic content and distillation properties of gasolines available in the U.S. (or in the case of LEV III, the state of California) more closely. The reduced aromatic content of Tier 3 and LEV III fuels also reduces carbon content relative to Tier 2 fuels.

Any analysis of future hardware technology packages must not be overly sensitive to fuel octane to account for manufacturers choosing to require use of “regular grade” (87 AKI minimum) gasoline during in-use operation of their vehicles. If the application were designated by the manufacturer for minimum 91 AKI gasoline, then there could be an unacceptable engine power de-rate if a consumer used regular grade gasoline

TABLE 5 Fuel specifications.

	EPA Tier II Certification Fuel	LEV III Regular Certification Fuel
Fuel Grade	Premium	Regular
Ethanol Content (vol %)	0	10
LHV (MJ/kg)	43.25	41.39
RON/MON/AKI	96 / 87.7 / 91.9	91.8 / 84.2 / 88.0
H:C	1.85	1.95
O:C	NA	0.0326
Total Aromatics (vol %)	28	22

Notes: LHV – Lower Heating Value, RON – Research Octane Number, MON – Motor Octane Number, AKI = (RON + MON)/2

rather than premium grade gasoline. EPA analyses of future technologies and strategies are therefore limited to operation on regular-grade fuel for wide appeal [20, 21]. Regular grade fuel (88 AKI E10) was simulated to investigate if a power de-rate was required and to quantify any resulting increase in fuel consumption. Fuel specifications for a LEV III fuel were used to match the fuel used for previous testing of this engine [1].

The simulation was repeated at the same compression ratio but with fuel properties from the ‘Regular’ fuel. Importantly, the VNT could still achieve the target load on regular grade fuel (Figure 27). The knock model accounted for fuel octane rating and retarded combustion phasing (Figure 28). Eight degrees or more of CA50 retard was required when operating on regular fuel.

The stability limit of the engine was assumed to occur at a CA50 of 30° after top dead center (aTDC) with moderate EGR rates. This estimate was based on test data [1]. At higher engine speeds (above approximately 3500 rpm), the required knock-limited combustion phasing pushed beyond this stability limit, so EGR was reduced (Figure 29). An investigation identified that high backpressure at high power led to increased residuals and, thus, knock propensity. Recall the knock model was validated to premium fuel with the twin scroll turbocharger and remained unchanged for this VNT study. The larger baseline twin-scroll turbine size was not well suited to meet the low-speed torque target. The tuned VNT turbine was smaller to achieve the torque target, though the reduced size will lead to higher backpressure at high speed operation.

FIGURE 27 Full Load Curve of simulations with premium and regular fuel.

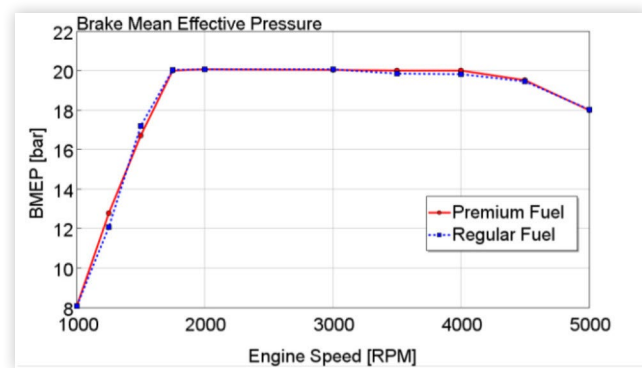


FIGURE 28 CA50 MFB for premium and regular fuel.

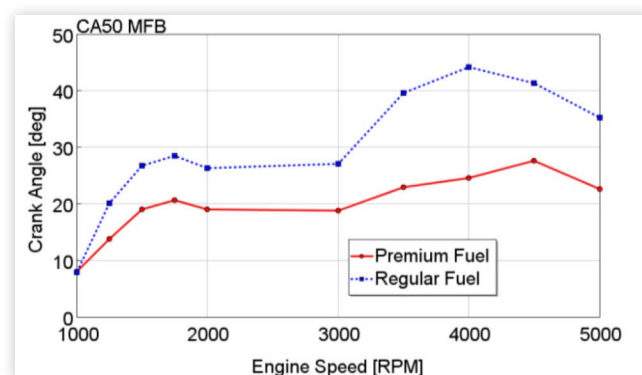
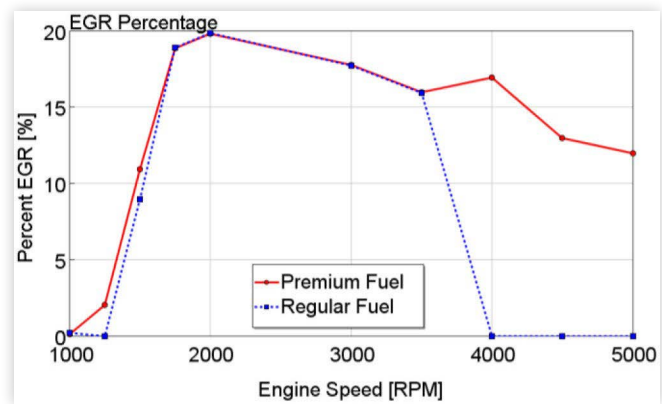


FIGURE 29 EGR percentage for premium and regular fuel.



The late combustion phasing had a significant negative impact on brake thermal efficiency (BTE), (Figure 30). At speeds below 3000 rpm, the EGR rates are the same, and only slight penalties are observed in BTE from the ~8° later CA50. Above 3000 RPM, combustion phasing retard and decreased EGR rate led to an efficiency drop and increased exhaust temperatures. Further enrichment was required to maintain appropriate pre-turbine temperatures, (Figure 31). A lambda of 0.73 is likely near the acceptable limit for production enrichment.

The lower efficiency demands higher airflow and intake manifold pressure to meet the target load (Figure 32). The higher airflow coupled with the later combustion drives increases pre-turbine pressure despite lower EGR rates (Figure 33).

BSFC across the operating range is plotted in Figure 34. A comparison to the premium fuel testing was performed on a BTE basis to account for the different lower heating values of the two fuels. (Figure 35) illustrates the large operating region where there is a slight difference: loads up to 12–14 bar BMEP. Most drive cycle operation occurs in the low-load (e.g., less than 12 bar BMEP), low-speed region (e.g., below 3000 rpm, depending on gearing), so drive cycle performance is unlikely to be significantly impacted.

Though the thermal efficiency of the regular fuel was no different for drive cycle operation, the lower-carbon-content LEV III E10 fuel has a positive impact on CO₂ emissions (Figure 36). The results indicated a brake-specific CO₂ (BSCO₂) benefit with regular fuel up to 13–15 bar BMEP. Above this

FIGURE 30 Brake thermal efficiency simulations results for premium and regular fuel.

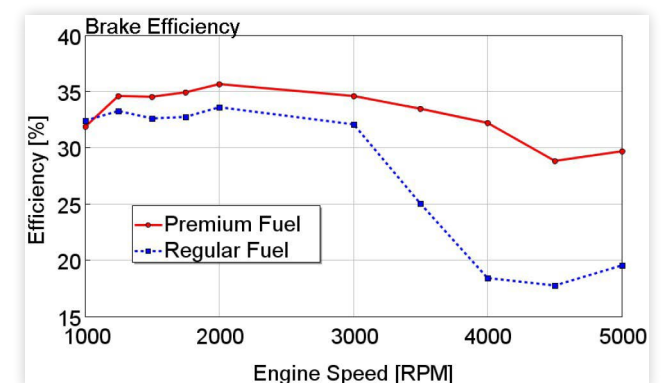


FIGURE 31 Lambda comparison between premium and regular fuel.

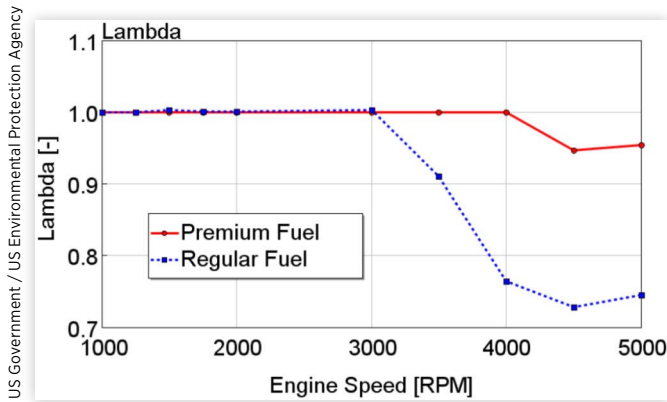


FIGURE 32 Intake manifold comparison between the premium and regular fuel.

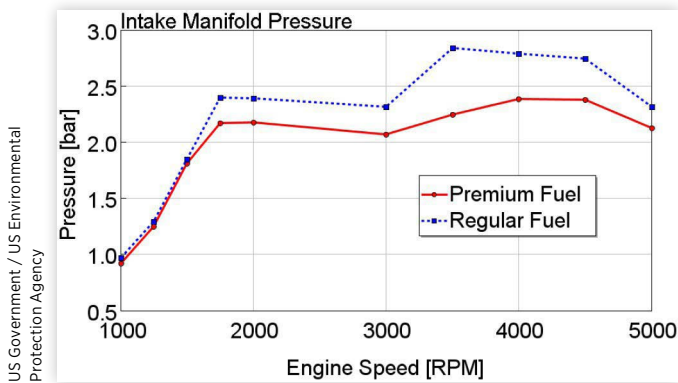


FIGURE 33 Simulation results for exhaust manifold backpressure for premium and regular fuels.

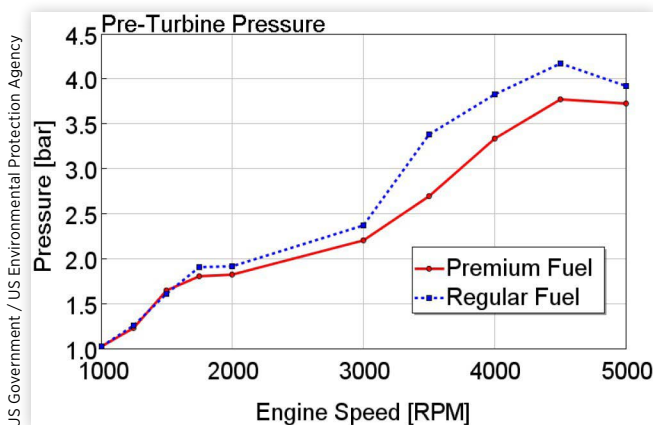


FIGURE 34 BSFC of regular fuel VNT with EGR.

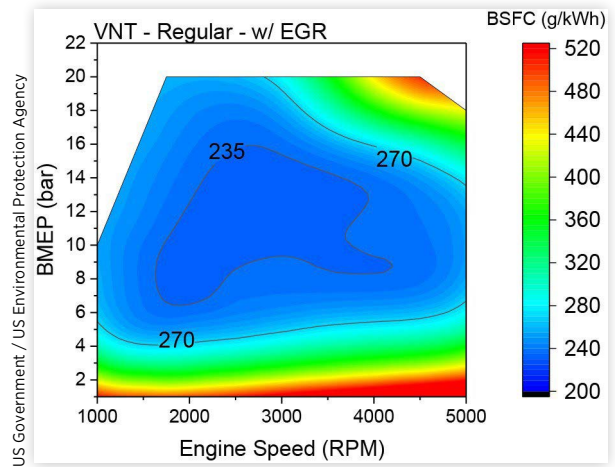


FIGURE 35 BTE difference between regular and premium fuel simulation results. A lower value indicates worse BTE for the regular fuel.

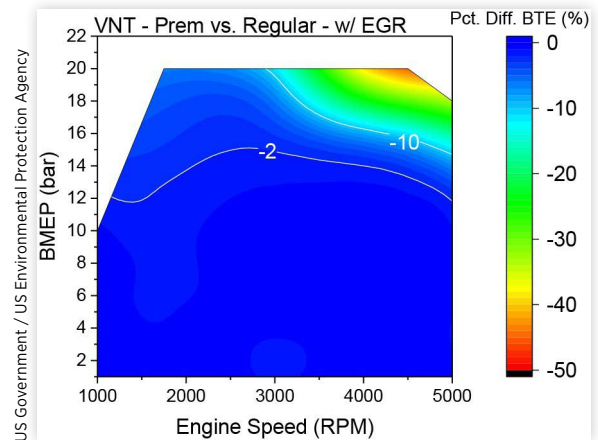


FIGURE 36 Comparison of predicted brake-specific CO₂ emissions between regular and premium fuels.

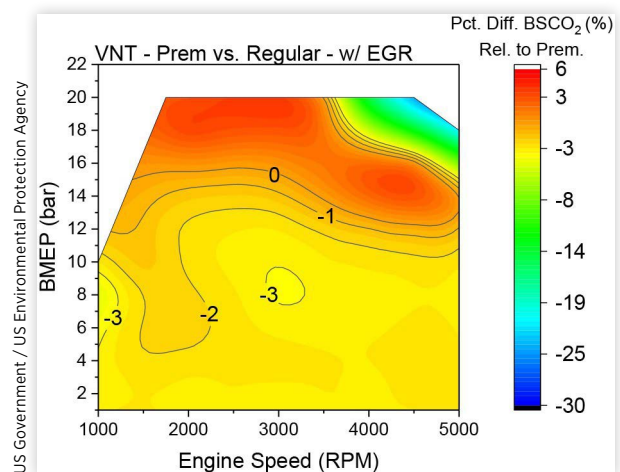
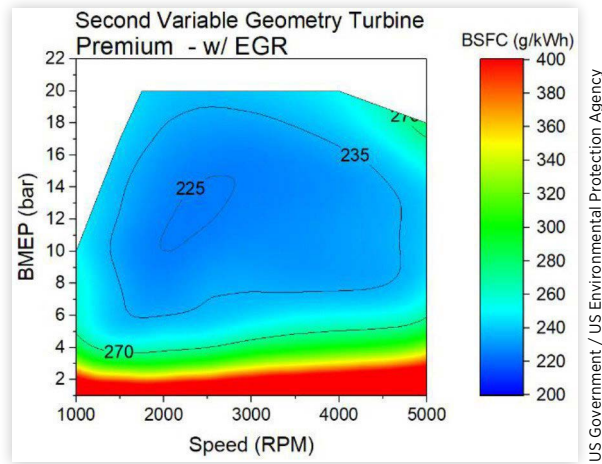


FIGURE 37 BSFC map of second Variable Geometry Turbine device.



load, the reduced efficiency from late combustion phasing offset the benefit from the carbon content of the fuel. Near peak power, however, there is a dramatic reduction in BSFC_{CO₂} resulting from the ~30% enrichment. Carbon monoxide emissions increased to ~500 g/kWh, offsetting BSFC_{CO₂} production.

Other Hardware Investigations

The created GT-Power model was also evaluated with hardware from another turbocharger supplier to corroborate the results presented in this paper.² The compressor and turbine maps for the other turbocharger were slightly larger. Both suppliers provided maps for existing hardware, and thus, only discrete steps between compressor and turbine sizes were available.

Both variable turbine turbochargers performed similarly. Each achieved the target load with similar EGR rates. BSFC values for most of the map matched each other, with only slight differences at some points (Figure 22, Figure 37). The comparable results from two model suppliers provides strong corroboration that a VNT is a viable solution to support LP-EGR across a wide range of engine operation.

Summary

A GT-Power model was created that used predictive knock and combustion sub-models. The model was initially tuned to match an EGR and non-EGR dataset and contour maps for three different model multipliers were produced. The model compared favorably to test data generated under sixteen sets of conditions with and without cooled LP-EGR. Generally, BSFC matched well to test data across the engine operating map with <2% absolute error being observed.

² Identification, turbine map and compressor map withheld at the request of the manufacturer.

Compressor and turbocharger maps of VNT technology were provided for this study and imported into the GT-Power model. The model was exercised on both regular and premium grade fuels.

Conclusions

Based on the simulation study carried out, the following conclusions are offered:

- Performance of the VNT was favorable at engine speeds below 3500 RPM and loads below 12 bar BMEP but higher back pressure resulted in reduced efficiency at higher speeds. For this study, the turbine required high efficiency at low flow capacity to act as the sole boost device and therefore had to be small enough to achieve the low speed, high load targets (1750 rpm 20 bar BMEP). Although BSFC increased marginally at the peak-power condition, it was possible to run the target torque curve with the single boost device.
- The GT-Power model appropriately retarded combustion phasing with regular grade fuel. EGR was removed to enable further spark retardation without combustion becoming unstable. The retarded combustion and removal of dilution increased exhaust gas temperature significantly, requiring further fuel addition to maintain <950 °C exhaust temperatures. Therefore, although the target torque curve could be achieved, efficiency was reduced. Efficiency performance was no different than the premium fuel results up to ~12 bar BMEP.
- The simulation effort was replicated on a different variable geometry turbine and the results were comparable to the first variable nozzle turbine study.
- The calibration maps for GT-Power SITurb model variables can be used to guide other modeling efforts which use high pressure dilute combustion.

Future Work

Future work intends to investigate the synergy between EGR and Miller operation with boost supplied from a VNT. The use of Miller strategy could compensate for the reduced knock resistance with the regular fuel and improve overall engine efficiency. It also has potential to reduce full load exhaust temperatures and resulting enrichment for component protection. The GT-Power *kinetics-fit-gasoline* model is also planned for future work to minimize ad hoc tuning as a function of EGR rate.

References

1. Conway, G., Robertson, D., Chadwell, C., Kargul, J. et al., "Evaluation of Emerging Technologies on a 1.6 L Turbocharged GDI Engine," SAE Technical Paper 2018-01-1423.

2. EPA Federal Register, "2017 and Later Model Year Light-Duty Vehicle Greenhouse Gas Emissions and Corporate Average Fuel Economy Standards," ISBN 7342144584: 62624-63200, 2012.
3. Yonekawa, A., Ueno, M., Watanabe, O., and Ishikawa, N., "Development of New Gasoline Engine for Accord Plug-in Hybrid," SAE Technical Paper [2013-01-1738](https://doi.org/10.4271/2013-01-1738), 2013, doi:[10.4271/2013-01-1738](https://doi.org/10.4271/2013-01-1738).
4. Gukelberger, R., Gingrich, J., Alger, T., Almaraz, S. et al., "LPL EGR and D-EGR® Engine Concept Comparison Part 1: Part Load Operation," *SAE Int. J. Engines* 8(2):570-582, 2015, doi:[10.4271/2015-01-0783](https://doi.org/10.4271/2015-01-0783).
5. Liu, Z. and Cleary, D., "Fuel Consumption Evaluation of Cooled External EGR for a Downsized Boosted SIDI DICP Engine," SAE Technical Paper [2014-01-1235](https://doi.org/10.4271/2014-01-1235), 2014, doi:[10.4271/2014-01-1235](https://doi.org/10.4271/2014-01-1235).
6. Song, D., Jia, N., Guo, X., Ma, X. et al., "Low Pressure Cooled EGR for Improved Fuel Economy on a Turbocharged PFI Gasoline Engine," SAE Technical Paper [2014-01-1240](https://doi.org/10.4271/2014-01-1240), 2014, doi:[10.4271/2014-01-1240](https://doi.org/10.4271/2014-01-1240).
7. Alger, T., Gingrich, J., Khalek, I., and Mangold, B., "The Role of EGR in PM Emissions from Gasoline Engines," *SAE Int. J. Fuels Lubr.* 3(1):85-98, 2010, doi:[10.4271/2010-01-0353](https://doi.org/10.4271/2010-01-0353).
8. Glahn, C., Kluin, M., Hermann, I., and Koenigstein, A., "980 °C Gasoline Variable Turbine Geometry – The Affordable Upcoming Technology for High-Volume Efficient Engines," in 26th Aachen Colloquium Automobile and Engine Technology, Oct. 20, 2017.
9. Bontemps, N., Roux, J.-S., and Jeckel, D., Schlosshauer, A. "VNT Turbocharger for Gasoline "Miller" Engines," in International Conference and Exhibition SIA Powertrain Versailles 2017, June 07, 2017.
10. Eichler, F., Demmelbauer-Ebner, W., and Theobald, J., Stiebels, B., "The New EA211 TSI Evo from Volkswagen," Proceedings: International Vienna Motor Symposium, 2016.
11. Roth, D., Keller, P., and Becker, M., "Requirements of External EGR Systems for Dual Cam Phaser Turbo GDI Engines," SAE Technical Paper [2010-01-0588](https://doi.org/10.4271/2010-01-0588), 2010, doi:<https://doi.org/10.4271/2010-01-0588>.
12. Wiebe, I.I., "Progress in Engine Cycle Analysis: Combustion Rate and Cycle Processes." Mashgiz, Ural-Siberia Branch, 1962, 271 pp (in Russian).
13. Wiebe, I. I. "Semi-empirical expression for combustion rate in engines." Proceedings of Conference on Piston engines, USSR, 1956, pp. 185-191. (Academy of Sciences, Moscow).
14. Ghojel, J., "Review of the Development and Applications of the Wiebe Function: A Tribute to the Contribution of Ivan Wiebe to Engine Research," *International Journal of Engine Research*. 11:297, 2010, doi:[10.1243/14680874JER06510](https://doi.org/10.1243/14680874JER06510).
15. Gillespie, L., Lawes, M., Sheppard, C., and Woolley, R., "Aspects of Laminar and Turbulent Burning Velocity Relevant to SI Engines," SAE Technical Paper [2000-01-0192](https://doi.org/10.4271/2000-01-0192), 2000, doi:<https://doi.org/10.4271/2000-01-0192>.
16. Livengood, J.C., and Wu, P.C., "Correlation of Autoignition Phenomena in Internal Combustion engines and Rapid Compression Machines," Fifth Symposium (International) on Combustion (1955) pp. 347-356.
17. Douaud, A. and Eyzat, P., "Four-Octane-Number Method for Predicting the Anti-Knock Behavior of Fuels and Engines," SAE Technical Paper [780080](https://doi.org/10.4271/780080), 1978, doi:<https://doi.org/10.4271/780080>.
18. Chen, S.K. and Flynn, P.F., "Development of Single Cylinder Compression Ignition Research Engine," SAE Technical Paper [650733](https://doi.org/10.4271/650733), 1965.
19. California Environmental Protection Agency – Air Resources Board. "California 2015 And Subsequent Model Criteria Pollutant Exhaust Emission Standards and Test Procedures and 2017 and Subsequent Model Greenhouse Gas Exhaust Emission Standards and Test Procedures for Passenger Cars, Light-Duty Trucks, and Medium-Duty Vehicles." §100.3.1.2 Certification Gasoline Fuel Specifications for LEV III Light-Duty Vehicles and Medium-Duty Vehicles. September 2, 2015 https://www.arb.ca.gov/msprog/levprog/cleandoc/ldtps_2015+_cp_or_2017+_ghg_my_lev%20iii_clean%20complete_10-15.pdf, last accessed Jan. 3, 2018.
20. U.S. EPA, "Proposed Determination on the Appropriateness of the Model Year 2022-2025 Light-Duty Vehicle Greenhouse Gas Emissions Standards under the Midterm Evaluation: Technical Support Document," EPA-420-R-16-020, November, 2016.
21. U.S. EPA, "Draft Technical Assessment Report: Midterm Evaluation of Light-Duty Vehicle Greenhouse Gas Emission Standards and Corporate Average Fuel Economy Standards for Model Years 2022-2025," EPA-420-D-16-901, July, 2016.

Contact Information

For additional information please contact **Graham Conway** at Southwest Research Institute at graham.conway@swri.org

Disclaimer

The views expressed in this article are those of the authors and do not necessarily represent the views or policies of the U.S. Environmental Protection Agency.

Acknowledgments

The authors would like to acknowledge Honeywell Transportation Systems for their technical support on this project and for providing VNT compressor and turbine map data.

Work by SwRI presented within this paper was conducted under contract to the U.S. EPA, Contract Number EP-C-15-006.

Definitions/Abbreviations

AKI - Anti-knock index

aTDC - After top dead center

BMEP - Brake mean effective pressure

BSCO₂ - Brake specific carbon dioxide

BSFC - Brake specific fuel consumption

BTE - Brake thermal efficiency

CA - Crank angle

CO₂ - Carbon dioxide

CR - Compression ratio

DI - Direct injection

EGR - Exhaust gas recirculation

FKGM - Flame kernel growth multiplier

GDI - Gasoline direct injection

GT - Gamma Technologies

LHV - Lower heating value

LP-EGR - Low-pressure EGR

MBT - Minimum spark advance for best torque

MFB - Mass fraction burned

MON - Motor Octane Number

NO_x - Oxides of nitrogen

RON - Research octane number

STL - Stereolithography

SwRI - Southwest Research Institute

TFSM - Turbulent flame speed multiplier

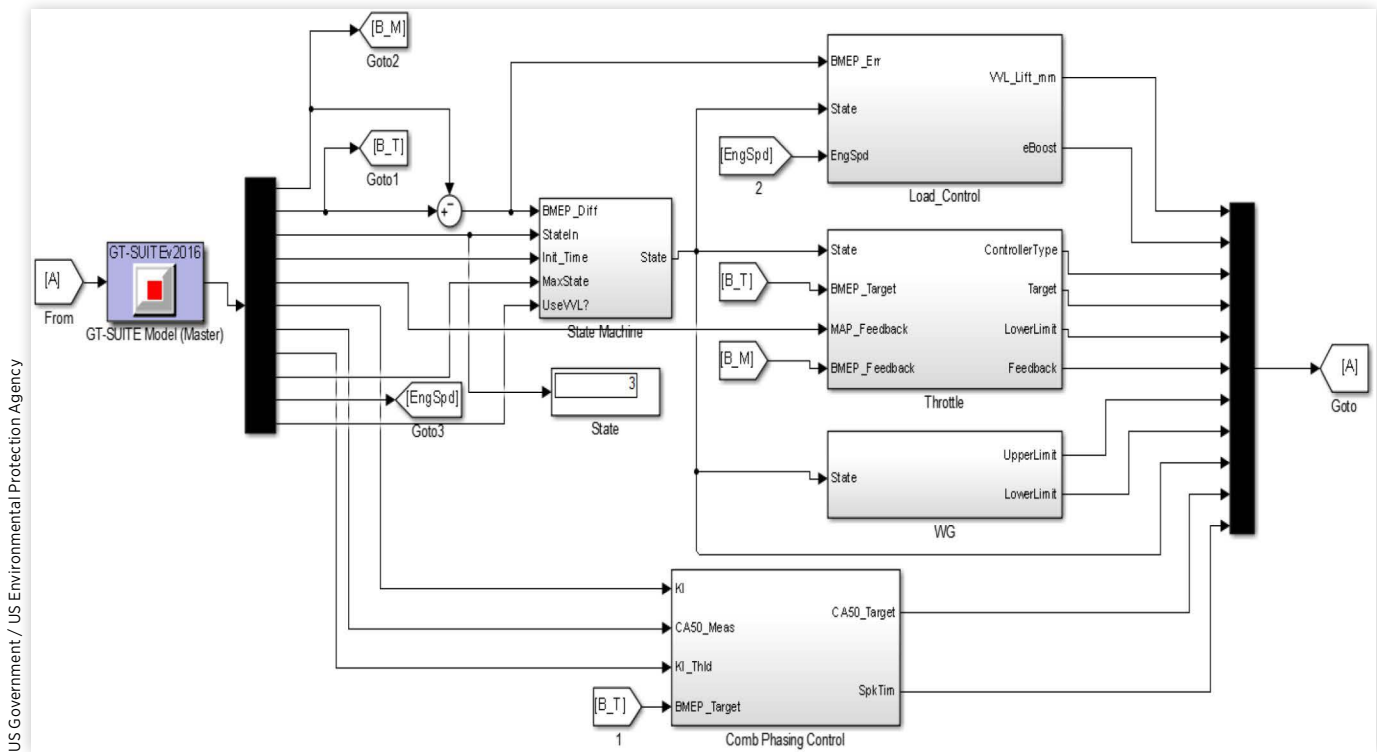
TWC - Three-way-catalyst

VNT - Variable nozzle turbocharger

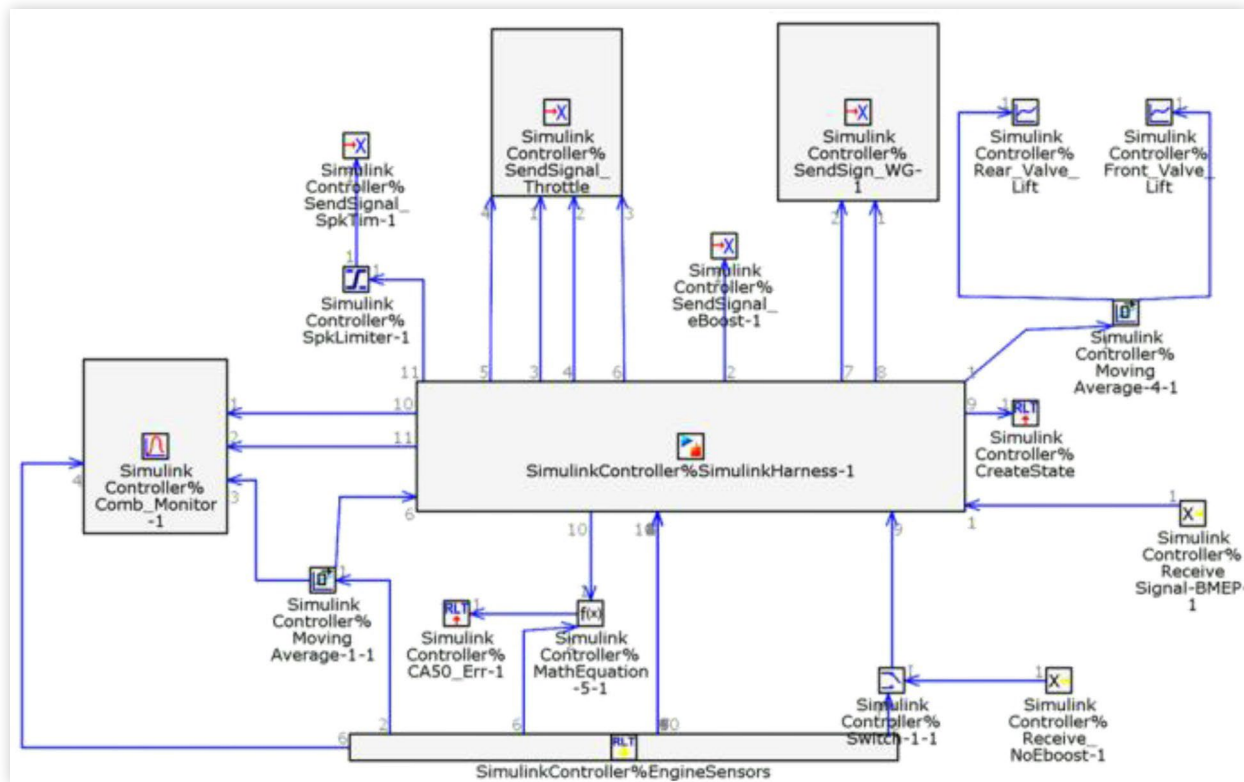
VVL - Variable valve lift

Appendix

APPENDIX FIGURE 1 Simulink control code.



US Government / US Environmental Protection Agency

APPENDIX FIGURE 2 SimulinkHarness object in GT-Power.

US Government / US Environmental Protection Agency

This is a declared work of the U.S. Government and is not subject to U.S. copyright protection. Foreign copyrights may apply. The U.S. Government assumes no liability or responsibility for the contents of this paper or the use of this paper, nor is it endorsing any manufacturers, products, or services cited herein and any trade name that may appear in the paper has been included only because it is essential to the contents of the paper.

Positions and opinions advanced in this paper are those of the author(s) and not necessarily those of SAE International. The author is solely responsible for the content of the paper.